NUMERICAL STUDY ON CHARACTERISTICS OF COMBUSTION AND POLLUTANT FORMATION IN A REHEATING FURNACE

by

Fengsheng QI[a*], Zisong WANG[a], Baokuan LI[a], Zhu HE[b], Jakov BALETA[c], and Milan VUJANOVIC[c]

[a] School of Metallurgy, Northeastern University, Shenyang, China
[b] Key Laboratory for Ferrous Metallurgy and Resources Utilization of Ministry of Education, Wuhan University of Science and Technology, Wuhan, China
[c] Department of Energy, Power Engineering and Environment, Faculty of Mechanical Engineering and Naval Architecture, University of Zagreb, Zagreb, Croatia

Original scientific paper
https://doi.org/10.2298/TSCI180118277Q

Energy consumption of fuel-fired industrial furnace accounts for about 23% of the national total energy consumption every year in China. Meanwhile, the reduction of combustion-generated pollutants in furnace has become very important due to the stringent environment laws and policy introduced in the recent years. It is therefore a great challenge for the researchers to simultaneously enhance the fuel efficiency of the furnace while controlling the pollution emission. In this study, a transient 3-D mathematical combustion model coupled with heat transfer and pollution formation model of a walking-beam-type reheating furnace has been developed to simulate the essential combustion, and pollution distribution in the furnace. Based on this model, considering nitrogen oxides formation mechanism, sensitivity study has been carried out to investigate the influence of fuel flow rate, air-fuel ratio on the resultant concentration of nitrogen oxides in the flue gas. The results of present study provide valuable information for improving the thermal efficiency and pollutant control of reheating furnace.

Key words: *energy consumption, reheating furnace, combustion, pollutant formation, nitrogen oxides emissions*

Introduction

In 2016, China's crude steel output was 808 million tons, the comprehensive energy consumption of per ton steel iron and steel industry was recorded as 572 kg(ce)/t (kg of coal equivalent per tone). Obviously, energy saving is one of the challenging tasks of the Chinese steel enterprises. On the other hand, as China's environmental pollution problem has increasingly become serious in recent years, environmental protection is another big challenge for China. Reheating furnace is one the most important equipment in the steel rolling process. The energy consumption of reheating furnace accounts for about 25% of total energy consumption of steel industry [1]. So, the improvement of energy efficiency of reheating furnace is very important for energy conservation and emissions reduction. The NO_x emission is one of mainly pollutant emissions of reheating furnace because the high combustion temperature. A great deal of attention is required to enhance the operating performance and to reduce NO_x emission of reheating furnace.

* Corresponding author; e-mail: qifs@mail.neu.edu.cn

Many efforts have been done to reveal the physical and chemical characteristics in the reheating furnace. Some mathematical models were developed to study the radiation heat transfer in reheating furnace. In the early stage, a push-type reheating furnace was divided into sub-zones, at each zone, only radiative heat transfer was considered, and temperatures of the medium and the wall for each sub-zone were set to fixed value [2]. After that, a series of CFD models were preformed to predict the temperature distribution in the furnace and the slabs, these models can be used for accurate prediction of the thermal, combustion and flow characteristics in the furnace, but there existed such difficulties as treatment of so many governing equations and complexity of the furnace structure as well as uncertainty of the models, therefore, it necessitates long computational time and costs [3-5]. Han *et al.* [6-9] have made outstanding contributions on transient radiative heating characteristics inside the reheating furnace. In their study, the thermal efficiency of a reheating furnace was predicted by considering radiative heat transfer to the slabs and the furnace wall. Furthermore, the effect of various fuel mixtures on the performance of a reheating furnace was also investigated. With the development of computational hardware and numerical methods, analysis of combustion process in reheating furnace has been performed. Zhang *et al.* [10] developed a numerical model to calculate the combustion process in a regenerative reheating furnace with the commercial software FLUENT. In their study, the geometry of the furnace was simplified as a rectangle. Stockwell *et al.* [11] have built a numerical model to predict the combustion process in an experimental regenerative reheating furnace. The predicted results were compared against experimental measurements. Other researchers [12, 13] have used another commercial computational fluid dynamics software package, PHOENICS to develop a 3-D model of pusher-type slab reheating furnace to gain knowledge of gas flows and temperature distribution in the furnace. Harish *et al.* [14] have presented a computational model for the heat transfer in a direct-fired pusher type reheating furnace by using the finite volume method for gas radiative heat transfer and weighted-sum-of-gray-gases model for non-gray behavior of the combustion gases within the furnace. Hsieh *et al.* [15] have investigated the turbulent reactive flow and radiative heat transfer problem in a walking-beam-type slab reheating furnace by the commercial software STAR-CD. Their model considers the whole furnace, including the burners, the walking-beam system with skid buttons, the slabs, the dams, and the down-take outlet. Wang *et al.* [16] developed a CFD model to analyze the slab heating characteristics in a reheating furnace where the probability density function model were used to simulate the combustion process in the reheating furnace. So far, the prediction of NO emission in heating furnace has not been reported. Some researchers have studied NO_x emissions from other industrial furnaces. Ishii *et al.* [17] have built a numerical model to investigate the NO_x emissions in a regenerative furnace, in this model three chemical kinetic processes for NO_x formation are included. Khalilarya and Lotfiani [18] have provided a numerical study of flow pattern and its effect on NO_x emissions in a single chamber square tangentially fired furnace. The combustion process has simulated using a global on-step reaction mechanism and the turbulence-chemistry interaction has been taken into account using the eddy-dissipation model.

In this study, a transient 3-D mathematical combustion model coupled with the pollution formation model in a walking-beam-type reheating furnace has been developed to study the combustion and temperature distribution in the furnace. Based on this model, considering NO_x formation mechanism, the influence of fuel flow rate, air-fuel ratio on the concentration of NO_x in flue gas has been investigated. The results are of great significance for the control of combustion and heat transfer in the heating furnace and the reduction of NO_x emission.

Mathematical model

The function of the reheating furnace is to heat steel slabs nearly up to 1,250 °C uniformly for the subsequent rolling process. At present, there are two types of commonly used slab-reheating furnaces; the pusher type and the walking-beam type. For the walking-beam type reheating furnace, the energy for slab heating is supplied by the roof and side gas burners. The combustion process of a walking-beam reheating furnace involves complex physical and chemical processes, including turbulent flow, chemical reaction, heat transfer, species transport and so on. This study aims to develop a comprehensive numerical model that considers all the relevant physical and chemical considerations in a walking-beam type reheating furnace. The numerical model was developed based on the commercial CFD package ANSYS FLUENT. Bases on the framework of the software, the following conservation equations were considered.

Turbulent combustion model

The equations that govern the conservation of mass, momentum, and energy, as well as the equations of species transport, can be expressed in the following general form:

$$\frac{\partial}{\partial t}(\rho\Phi)+\frac{\partial}{\partial x_i}(\rho u_i\Phi)=\frac{\partial}{\partial x_i}\left(\Gamma_\Phi\frac{\partial\Phi}{\partial x_i}\right)+S_\Phi \tag{1}$$

When Φ = 1, equations stands for the continuity equation. While a substitution of velocity components in to Φ generates the momentum equation for each respective direction. The enthalpy conservation equation can be obtained when the mixture enthalpy is substituted into Φ. When the mass fraction Y_i is substituted into Φ, the conservation equation of species mass fraction is obtained. In the equation, the density ρ is determined by incompressible-ideal-gas law.

It is well known that the realizable k-ε turbulence model is relatively stable, robust and computationally efficient. Therefore, the realizable k-ε turbulence model was used to simulate the turbulent flow in this study. The P-1 model gives good results in many circumstances without making the problem computationally intensive, and it takes into account the effects of scattering. So, the P-1 model was used to calculate the radiation heat transfer in present study. In this study, reaction rates are assumed to be controlled by turbulent mixing, the effect of chemistry timescales is ignored, and so expensive Arrhenius chemical kinetics calculations are avoided. The combustion is modeled using a global one-step reaction mechanism, turbulence-chemistry interaction is considered using the eddy-dissipation model.

The NO modeling

The NO_x formation and destruction process in combustion systems are very complex phenomenon. During the combustion reaction, nitrogen either in the air or in the fuel is converted to nitrogen-containing pollutants such as NO, NO_2, nitrous oxide (N_2O), ammonia (NH_3) and hydrogen cyanide (HCN). The pollutants depend on the temperature and species of the fuel. The processes are highly complex, involving a large number of inter mediate species. However, in this study, only a few global steps are considered for simulation NO_x formation to facilitate their interaction with velocity, temperature and concentration field. The transport equation of NO is given:

$$\frac{\partial}{\partial t}(\rho Y_{\mathrm{NO}})\frac{\partial}{\partial x_i}(\rho u_i Y_{\mathrm{NO}})=\frac{\partial}{\partial x_i}\left(\rho D_{\mathrm{NO}}\frac{\partial Y_{\mathrm{NO}}}{\partial x_i}\right)+S_{\mathrm{NO}} \tag{2}$$

where D_{NO} is the effective diffusion coefficient and S_{NO} − the source term, which is determined by different NO_x generation mechanism. The thermal NO_x and prompt NO_x are considered in this study.

For the thermal NO_x mechanism:

$$S_{\text{thermal,NO}} = M_{\omega,\text{NO}} \frac{\text{d}[\text{NO}]_{\text{thermal}}}{\text{d}t} \tag{3}$$

The thermal NO_x rate of formation/destruction is significant at high temperature, it can be determined by the extended Zeldovich mechanism. The net rate of formation/destruction is given [18]:

$$\frac{\text{d}[\text{NO}]_{\text{thermal}}}{\text{d}t} = 2k_{f,1}[\text{O}][\text{N}_2]\frac{1-\dfrac{k_{r,1},k_{r,2}[\text{NO}]^2}{k_{f,1}[\text{N}_2]k_{f,2}[\text{O}_2]}}{1+\dfrac{k_{r,1}[\text{NO}]}{k_{f,2}[\text{O}_2]+k_{f,3}[\text{OH}]}} \tag{4}$$

where $[\text{O}] = 36.64\, T^{1/2}\,[\text{O}_2]^{1/2}\,\text{e}^{-27,123/T}$ mol/m^3.

For the prompt NO_x mechanism:

$$S_{\text{prompt,NO}} = M_{\omega,\text{NO}} \frac{\text{d}[\text{NO}]_{\text{prompt}}}{\text{d}t} \tag{5}$$

A modified De Soete model has been used in present simulation [17, 19]. A correction fator (F) which incorporates the effect of number of carbon atoms and the air-fuel ratio:

$$\frac{\text{d}[\text{NO}]_{\text{prompt}}}{\text{d}t} = Fk'_{pr}[\text{O}_2]^a[\text{N}_2][\text{FUEL}]\text{e}^{-E'_a/\text{RT}} \tag{6}$$

$$F = 4.75 + 0.0819n - 23.2\psi + 32\psi^2 - 12.2\psi^3 \tag{7}$$

$$k'_{pr} = 6.4\cdot 10^6\left(\frac{\text{R}T}{p}\right)^{a+1} \tag{8}$$

where E_a is 303,474.125 J/mol, n is the number of carbon atoms per molecule, and Ψ is equivalence ratio. The oxygen reaction order a depends on flame conditions and can be calculated by oxygen mole fraction in the flame:

$$a = \begin{cases} 1.0, & X_{\text{O}_2} \le 4.1\cdot 10^{-3} \\ -3.95 - 0.9\ln X_{\text{O}_2}, & 4.1\cdot 10^{-3} \le X_{\text{O}_2} \le 1.11\cdot 10^{-2} \\ -0.35 - 0.1\ln X_{\text{O}_2}, & 1.11\cdot 10^{-2} \le X_{\text{O}_2} \le 0.03 \\ 0, & X_{\text{O}_2} \ge 0.03 \end{cases} \tag{9}$$

Computational domain and mesh generation

Figure 1 shows the schematic of the walk-beam reheating furnace which is simplified furnace model from a walk-beam type reheating furnace of one of Chinese steel enterprises. The dimensions of the furnace are 51.7 m × 11.7 m × 4.35 m and the furnace contains

35 slabs. The size of each slab is 10.5 m × 1.4 m × 0.23 m. This furnace can be divided into four zones:

– preheating zone,
– first heating zone,
– second heating zone, and
– soaking zone as shown in fig. 1(b).

A total of thirty flat burners were uniformly set on the top of the soaking zone, and other fifty-eight flame burners were set on the two sides of the furnace. Each burner is simplified with two concentric circles. The inner circle is used for fuel passage and the annulus formed by two concentric circles is used for air passage. For the flat burners, the diameter of the inner circle and the outer circle are 0.08 m and 0.18 m, respectively, for blame burners, the diameter of the inner circle and the outer circle are 0.18 m and 0.38 m, respectively.

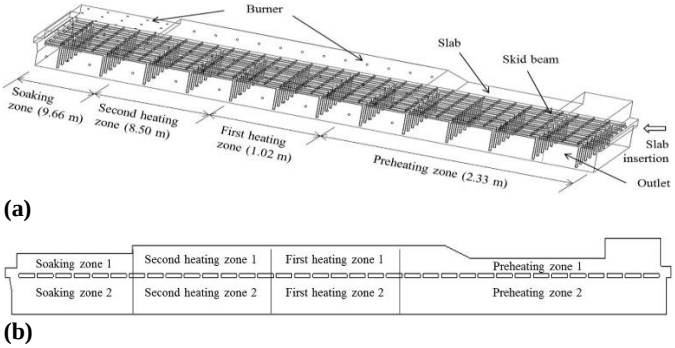

Figure 1. Schematic of the walk-beam reheating furnace; (a) 3-D view, (b) cross-section

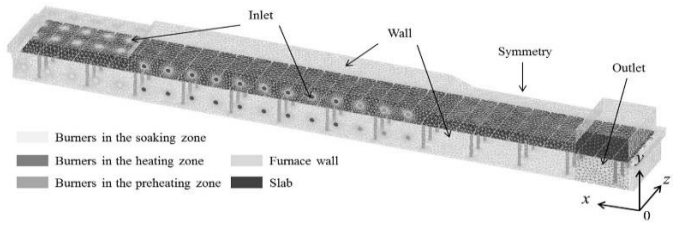

Figure 2. Grids of the computational domain

As the furnace is symmetrical, in order to reduce the amount of calculation, half of the furnace was selected as computational domain. A hybrid structured and unstructured meshes were generated throughout the computational domain. As shown in fig. 2, local mesh refinements were also employed to capture the local flow structure and combustion process in the furnace. Based on the gird independence analysis, the final mesh with the total grid nodes of 4.32 million was used for numerical simulations.

Operation parameters and boundary conditions

All boundary conditions are set with reference to the typical operating parameters. The fuel is the mixture gas of blast furnace gas, coke oven gas, converter gas and nature gas. The fuel compositions are shown in tab. 1. Because the content of ethylene (C_2H_4) is very low, the conservation equation of CO, H_2, and CH_4 have been solved in this study. The furnace outlet is considered as pressure outlet. As mentioned before, half of the furnace was selected as computational domain, the symmetry surface is shown in fig. 2. The top wall, bottom wall and side walls are assumed as non-slip wall and the he heat flux of the walls set to 500 W/m^2 according to the experience. The skid beam wall was set as convection heat transfer boundary with convection heat transfer coefficient is 300 W/m^{2}K. Three inlet flow rates of the fuel were investigate in this study, they are 6900 Nm^3 per hours, 8600 Nm^3 per hours, and 10400 Nm^3 per hours. The air-fuel ratios were set as 1.05, 1.1, and 1.2, respectively.

Table 1. Composition of fuel

Species	CO	H_2	CH_4	C_2H_4	N_2	CO_2	O_2
Fraction	0.2708	0.1404	0.0772	0.0063	0.3491	0.1457	0.0104

Results and discussion

Model validation

Measurements from an on-site field test are used for model validation in present study. In the field test, eight thermocouples set on the upper and down regions of the wall were used to measure the temperature at different zones of the furnace. Table 2 shows the comparison between the simulated and measured temperature at the different testing locations when fuel flow rate is 8600 Nm^3/h and the air-fuel ratio is 1.1. As depicted, the predicted temperatures are well agreed with the measured results. The averaged prediction error is around 5% which shows the validity of the present numerical model in predicting temperature in the reheating furnace.

Table 2. Comparison of predict temperature with measurement data

Test point	Preheating zone 1	Preheating zone 2	First heating zone 1	First heating zone 2	Second heating zone 1	Second heating zone 2	Soaking zone 1	Soaking zone 2
Measured [°C]	1007.1	946.9	1161.0	1155.3	1191.2	1165.7	1134.6	1127.6
Predicted [°C]	1061.4	911.1	1214.5	1117.5	1157.4	1151.6	1061.9	1046.4
Relative error	+0.054	−0.038	+0.046	−0.033	−0.028	−0.012	−0.064	−0.072

Flow field and temperature distribution

In the rehearing furnace, the fuel gas is injected into the chamber from the flame burners on each side of the furnace. At the upper part of soaking zone, the flat flame burners were used. The flame structure of the flat flame burners looks like a disk, which can transfer the heat to the slabs uniformly. At the inlet of the flat flame burner, a swirling flow was occurred to form the big flat flame. Figures 3(a) and 3(b) show the flow field on different sections of the furnace. From fig. 3(b), it can be seen the fuel and air injected into the chamber and move to the outlet of the furnace. The higher velocities are located at the inlet and the middle of preheating zone. From fig. 3(a), it can be seen, at the down part of the combustion chamber, the velocity is smaller because the flowing area is larger than that at the upper parts. Furthermore, it is obvious that the velocity near the slabs is larger, that is very beneficial for convective heat transfer for slab.

Figures 4(a) and 4(b) show the temperature distribution of the furnace on plane z = 2.9 m and y = 3.35 m. From fig. 4(b), it can be observed that the fuel gas and air start to burn at the outlet of the burners. The mean temperature at soaking zones is about 1150 °C and temperature distribution is more uniform than other zones because the flat flame burner was used at the upper part of soaking zone, which can ensure the temperature of the heated slabs is uniform. The mean temperature in the first and second heating zones are about 1170 °C and 1180 °C, respectively. During the actual heating process, the slabs were heated rapidly in these zones. This furnace was designed to use the waste heat to preheat slabs, at the preheating zone only six burners were set. And the temperature at preheating zone is lowest.

Figures 5(a) and 5(b) show the temperature curves along the centerline of the furnace at different fuel flow rates and air-fuel ratio, respectively. It can be observed that with

the fuel flow rate increases from 6900 Nm^3 per hours to 10400 Nm^3 per hours, the temperature in the furnace increases about 120 °C. And with the air-fuel ratio increases from 1.05 to 1.2, the temperature in the furnace increases about 30 °C.

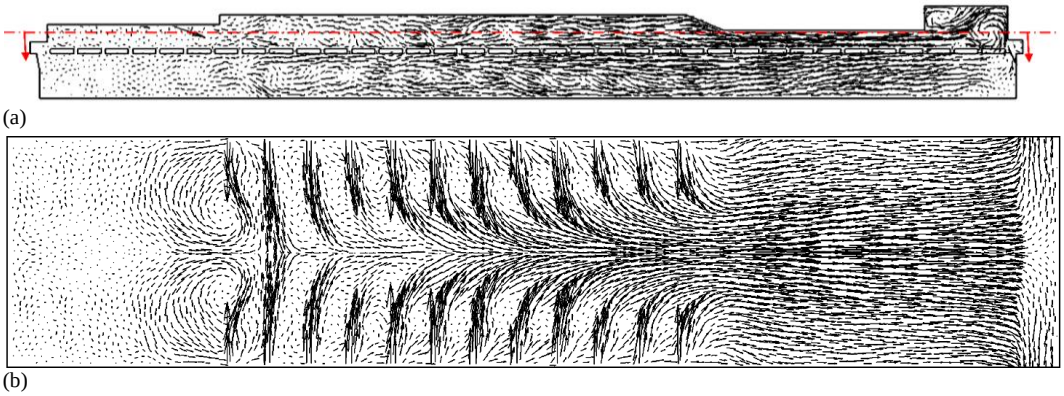

Figure 3. Flow field on different planes of the furnace; (a) z = 2.9 m, (b) y = 3.35 m

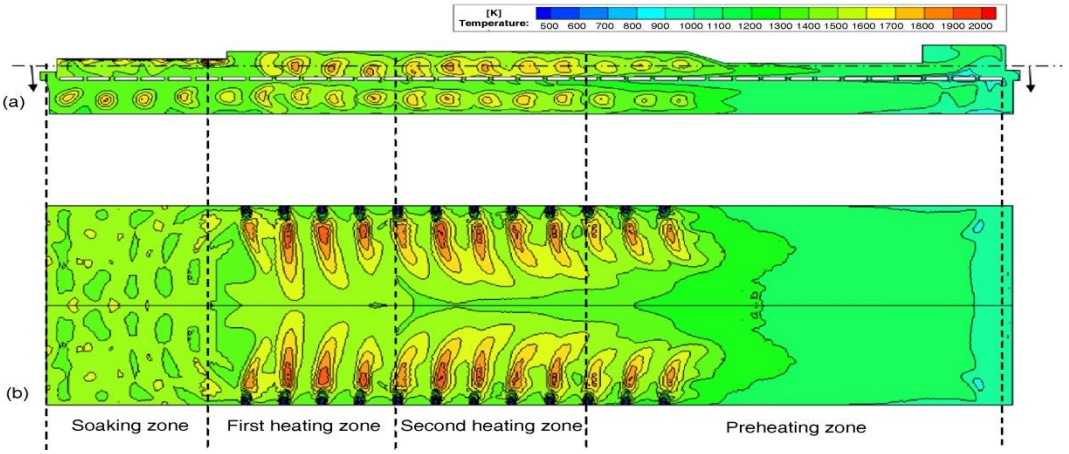

Figure 4. Temperature distribution of the furnace on different planes: (a) z = 2.9 m; (b) y = 3.35 m

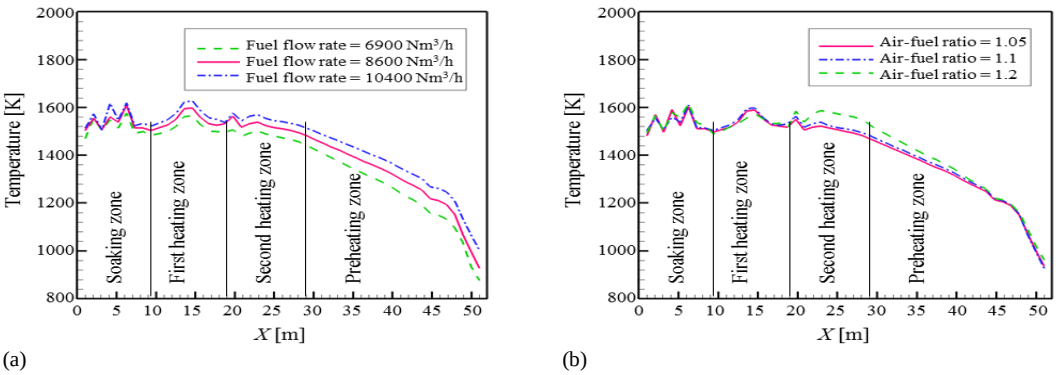

Figure 5. Temperature along the centerline of the furnace; (a) different fuel flow rates, (b) different air-fuel ratios

The NO_X distribution

High temperature in the furnace can generate the NO_x, and the main NO_x emission in a reheating furnace is NO. Figure 6 shows NO mass fraction on the section of y = 3.35 m. From the figures, it can be seen the NO concentration is very low at the out let of the furnace. Based on the Zeldovich theory, the thermal formation should be highly dependent on temperature. As the temperature greater than 1530 °C, the rate of thermal NO formation becomes larger suddenly, and it doubles for every 90 °C temperature increase beyond 1930 °C. But in this study, the temperature of the reheating furnace is below 1530 °C, so the thermal NO formation is not large. Furthermore, the NO mass fraction at soaking zone is smaller than that at first heating zones because the local high temperature occurs at heating zones, which leads to more NO generation. The prompt NO formation is mainly dependent on the fuel type and the oxygen concentration. Hydrocarbon fuels produce a large number of NO under a certain fuel-air ratio. In this study, the amount of CH_4 in the fuel is only 13%, so the prompt NO formation has little effect on the whole NO generation.

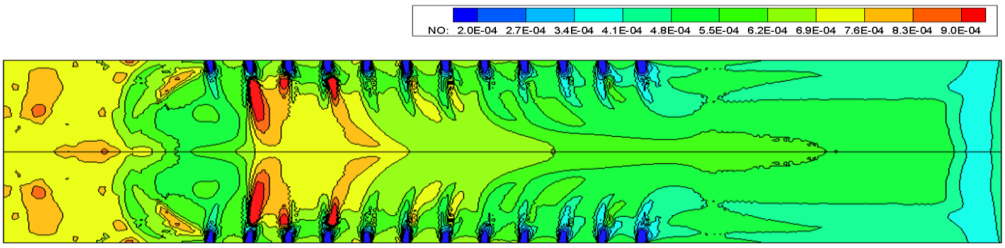

Figure 6. The NO mass fraction on the plane of y = 3.35 m

Figures 7(a) and 7(b) shows NO concentration along the furnace length direction at different fuel gas flow rates and different air-fuel ratios, respectively. With the fuel flow rate increasing from 6900 Nm^3 per hours to 10400 Nm^3 per hours, the concentration of NO increases about 30 mg/m^3, because with the fuel gas flow rate increasing, the temperature increases, high temperature results in high NO production. On the other hand, with the increasing of air-fuel ratio from 1.05 to 1.2, the concentration of NO increases about 6%. At large air-fuel ratio, the N_2 has more opportunities to react with O_2, and more NO generated. So, the air-fuel ratio should be strictly controlled in the actual production processes of reheating furnace.

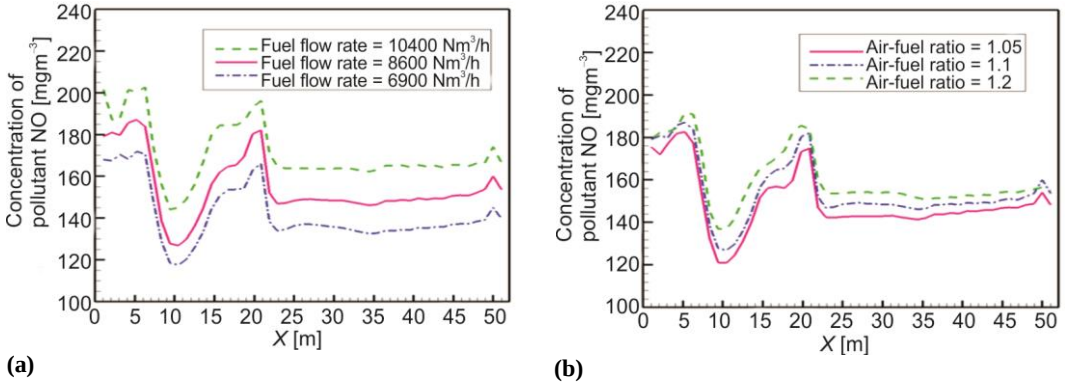

Figure 7. The NO concertation along the furnace: (a) at different fuel flow rate; (b) at different air-fuel ratio

Conclusion

In the present work, a transient 3-D mathematical combustion model coupled heat transfer and pollution formation model of a walking-beam-type reheating furnace has been developed. Using the model, the flow field, temperature distribution, the NO concentration of the reheating furnace can be obtained. Based on the predicted results, NO concentration in the furnace at different fuel flow rates and different air-fuel ratios have been analyzed. With the air-fuel ratio increasing from 1.05 to 1.2, the concentration of NO increases about 6%. The model and results of present study provide theory basis to the improvement of thermal efficiency and pollutant control of reheating furnace. The air-fuel ratio should be strictly controlled in the actual production processes of reheating furnace.

Acknowledgment

This work reported in this paper was supported by National Key R&D Program of China (2017YFB0304000) and the Open Research Fund of Key Laboratory for Ferrous Metallurgy and Resources Utilization of Ministry of Education, Wuhan University of Science and Technology (Grant No. FMRU201503).

Nomenclature

a – oxygen reaction order
D_{NO} – the effective diffusion coefficient
E_a – activation energy, [Jmol^{-1}]
F – correction factor
$k_{r,1}$, $k_{r,2}$ – kinetic rate constants, for reverse reactions
$k_{f,1}$, $k_{f,2}$, $k_{f,3}$ – kinetic rate constants, for forward reactions
$M_{\omega NO}$ – the molecular weight of NO, [kgmol^{-1}]
n – the number of carbon atoms per molecule
p – pressure, [Pa]
R – the universal gas constant
S_Φ – source term for various Φ
S_{NO} – source term for NO
$S_{prompt,NO}$ – source term for prompt NO
$S_{thermal,NO}$ – source term for thermal NO
T – temperature, [K]
t – time, [s]
u_i – velocity at different direction, [ms^{-1}]
x_i – Cartesian co-ordinates
Y_{NO} – the mass fraction of NO in the gas phase
[FUEL] – concentration of fuel, [molm^{-3}]
[N_2] – concentration of N_2, [molm^{-3}]
[O] – concentration of O atoms, [molm^{-3}]
[O_2] – concentration of O_2, [molm^{-3}]
[NO] – concentration of NO [molm^{-3}]
[OH] – concentration of free radical OH, [molm^{-3}]

Greek symbols

ρ – density, [kgm^{-3}]
Γ_Φ – the diffusion coefficient, [–]
ψ – equivalence ratio, [–]
Φ – the dependent variable, [–]

References

[1] Yao, W. L., Xing, T., Analysis of Energy Situation and Corresponding Strategy of China, *Energy Research and Information*, *22* (2006), 4, pp. 187-193
[2] Li, Z. Y., *et al.*, Computer Simulation of the Slab Reheating Furnace, *Canadian Metallurgical Quarterly*, *27* (1988), 3, pp. 187-196
[3] Kim, J. G., Huh, K. Y., Three Dimensional Analysis of the Walking Beam Type Reheating Furnace in Hot Strip Mills, *Numerical Heat Transfer, Part A*, *38* (2000), 7, pp. 589-609
[4] Kim, J. G., Huh, K. Y., Prediction of Transient Slab Temperature Distribution in the Reheating Furnace of a Walking-Beam Type for Rolling of Steel Slabs, *ISIJ International*, *40* (2000), 11, pp. 1115-1123
[5] Kim, M. Y., A Heat Transfer Model for the Analysis of Transient Heating of the Slab in a Direct-fired Walking Beam Type Reheating Furnace, *International Journal of Heat and Mass Transfer*, *50* (2007), 19-20, pp. 3740-3748
[6] Han, S. H., *et al.*, Transient Radiative Heating Characteristics of Slabs in a Walking Beam Type Reheating Furnace, *International Journal of Heat and Mass Transfer*, *52* (2009), 3-4, pp. 1005-1011

[7] Han, S. H., *et al.*, A Numerical Analysis of Slab Heating Characteristics in a Walking Beam Type Reheating Furnace, *International Journal of Heat and Mass Transfer*, *53* (2010), 19-20, pp. 3855-3861
[8] Han, S. H., *et al.*, Efficiency Analysis of Radiative Slab Heating in a Walking-beam-type Reheating Furnace, *Energy*, *36* (2011), 2, pp. 1265-1272
[9] Han, S. H., Chang, D. J., Radiative Slab Heating Analysis for Various Fuel Gas Compositions in an Axial-fired Reheating Furnace, *International Journal of Heat and Mass Transfer*, *55* (2012), 15-16, pp. 4029-4036
[10] Zhang, C., *et al.*, Numerical Modeling of the Thermal Performance of Regenerative Slab Reheat Furnaces, *Numerical Heat Transfer, Part A*, *66* (1997), 32, pp. 613-631
[11] Stockwell, N., *et al.*, Numerical Simulations of Turbulent Non-premixed Combustion in a Regenerative Furnace, *ISIJ International*, *41* (2001), 10, pp. 1272-1281
[12] Maki, A. M., *et al.*, Numerical Study of the Pusher-type Slab Reheating Furnace, *Scandinavian Journal of Metallurgy*, *31* (2002), 2, pp. 81-87
[13] Tang, Y., *et al.*, The Modeling of the Gas Flow and its Influence on the Scale Accumulation in the Steel Slab Pusher-Type Reheating Furnace, *ISIJ International*, *43* (2003), 11, pp. 1333-1341
[14] Harish, J., Dutta, P., Heat Transfer Analysis of Pusher Type Reheat Furnace, *Ironmaking Steelmaking*, *32* (2005), 2, pp. 151-158
[15] Hsieh, C. T., *et al.*, Numerical Modeling of a Walking-beam-type Slab Reheating Furnace, *Numerical Heat Transfer, Part A*, *53* (2008), 9, pp. 966-981
[16] Wang, J., *et al.*, Analysis of Slab Heating Characteristics in a Reheating Furnace, *Energy Conversion and Management*, *149* (2017), Oct., pp. 928-936
[17] Ishii, T., *et al.*, Effects of NO Models on the Prediction of NO Formation in a Regenerative Furnace, *Journal Energy Resources Technology*, *122* (2000), 4, pp. 224-228
[18] Khalilarya, S., Lotfiani, A., Determination of Flow Pattern and its Effect on NO_x Emission in a Tangentially Fired Single Chamber Square Furnace, *Thermal Science*, *14* (2010), 2, pp. 493-503
[19] DeSoete, G. G., Overall Reaction Rates of NO and Formation from Fuel Nitrogen, in: *15th Symp. on Combustion*, The Combustion Institute, 1975, pp. 1093-1102

Paper submitted: January 18, 2018
Paper revised: April 25, 2018
Paper accepted: April 25, 2018